Biochimica et Biophysica Acta 1842 (2014) 1413–1422

Contents lists available at ScienceDirect

Biochimica et Biophysica Acta

journal homepage: www.elsevier.com/locate/bbadis

Sulfite disrupts brain mitochondrial energy homeostasis and induces mitochondrial permeability transition pore opening *via* thiol group modification

Mateus Grings [a], Alana P. Moura [a], Alexandre U. Amaral [a], Belisa Parmeggiani [a], Juciano Gasparotto [a], José C.F. Moreira [a], Daniel P. Gelain [a], Angela T.S. Wyse [a], Moacir Wajner [a,b], Guilhian Leipnitz [a,*]

[a] Departamento de Bioquímica, Instituto de Ciências Básicas da Saúde, Universidade Federal do Rio Grande do Sul, Rua Ramiro Barcelos, 2600-Anexo, CEP 90035-003 Porto Alegre, RS, Brazil
[b] Serviço de Genética Médica, Hospital de Clínicas de Porto Alegre, Rua Ramiro Barcelos, 2350, CEP 90035-903 Porto Alegre, RS, Brazil

ARTICLE INFO

Article history:
Received 26 November 2013
Received in revised form 23 April 2014
Accepted 25 April 2014
Available online 2 May 2014

Keywords:
Sulfite oxidase deficiency
Sulfite
Bioenergetic dysfunction
Mitochondrial permeability transition
Calcium
Brain mitochondria

ABSTRACT

Sulfite oxidase (SO) deficiency is biochemically characterized by the accumulation of sulfite, thiosulfate and S-sulfocysteine in tissues and biological fluids of the affected patients. The main clinical symptoms include severe neurological dysfunction and brain abnormalities, whose pathophysiology is still unknown. The present study investigated the *in vitro* effects of sulfite and thiosulfate on mitochondrial homeostasis in rat brain mitochondria. It was verified that sulfite *per se*, but not thiosulfate, decreased state 3, CCCP-stimulated state and respiratory control ratio in mitochondria respiring with glutamate plus malate. In line with this, we found that sulfite inhibited the activities of glutamate and malate (MDH) dehydrogenases. In addition, sulfite decreased the activity of a commercial solution of MDH, that was prevented by antioxidants and dithiothreitol. Sulfite also induced mitochondrial swelling and reduced mitochondrial membrane potential, Ca^{2+} retention capacity, NAD(P)H pool and cytochrome *c* immunocontent when Ca^{2+} was present in the medium. These alterations were prevented by ruthenium red, cyclosporine A (CsA) and ADP, supporting the involvement of mitochondrial permeability transition (MPT) in these effects. We further observed that N-ethylmaleimide prevented the sulfite-elicited swelling and that sulfite decreased free thiol group content in brain mitochondria. These findings indicate that sulfite acts directly on MPT pore containing thiol groups. Finally, we verified that sulfite reduced cell viability in cerebral cortex slices and that this effect was prevented by CsA. Therefore, it may be presumed that disturbance of mitochondrial energy homeostasis and MPT induced by sulfite could be involved in the neuronal damage characteristic of SO deficiency.

1. Introduction

Sulfite, thiosulfate and S-sulfocysteine accumulate in tissues and biological fluids of patients affected by sulfite oxidase (SO) deficiency, an autosomal recessive disorder which can arise either from the isolated deficiency of the enzyme SO or from defects in the biosynthetic pathway of its essential cofactor, a molybdenum containing pterin molecule [1,2]. SO is a mitochondrial enzyme that catalyzes the final step in the oxidative degradation of the sulfur containing amino acids cysteine and methionine, playing also an important role in detoxifying exogenously supplied sulfite, since this metabolite may be generated from compounds that are used in food and pharmaceutical industries as preservatives and antimicrobial agents [3–5].

Both forms of SO deficiency are clinically characterized by progressive neurological dysfunction, severe neonatal seizures, lens subluxation, axial hypotonia, limb hypertonicity and failure to thrive, resulting often in early childhood death [1,2,6]. Neuropathological studies reveal severe encephalopathy with neuronal loss and demyelination in the cerebral white matter accompanied by gliosis and diffuse spongiosis. Marked atrophy of the cerebral cortex, basal ganglia, thalami, as well as myelin loss in the cerebellum are also reported [1,6–8]. Furthermore, MRI scans show hypoplasia of the corpus callosum, basal ganglia and brainstem, and cystic changes and calcifications in the basal ganglia [1,9].

Abbreviations: AASA, α-aminoadipic semialdehyde; ANT, adenine nucleotide translocator; Alam, alamethicin; BSA, bovine serum albumin; CAT, catalase; CCCP, carbonyl cyanide m-chlorophenyl hydrazine; CoQ, coenzyme Q_{10}; CP, chlorpromazine; CsA, cyclosporin A; DTT, dithiothreitol; FAU, fluorescence arbitratry units; FCCP, carbonyl cyanide-4-(trifluoromethoxy) phenylhydrazone; GDH, glutamate dehydrogenase; GM, glutamate plus malate; α-KG, α-ketoglutarate; α-KGDH, α-ketoglutarate dehydrogenase; MDH, malate dehydrogenase; MEL, melatonin; MPT, mitochondrial permeability transition; MTT, 3-(4,5-dimethylthiazol-2-yl)-2,5-diphenyltetrazolium bromide; NAC, N-acetylcysteine; NEM, N-ethylmaleimide; P6C, piperideine-6-carboxylate; PM, pyruvate plus malate; QUIN, quinacrine; RCR, respiratory control ratio; RR, ruthenium red; SO, sulfite oxidase; SUC, succinate; TFZ, trifluoperazine; TNB, 5-thio-2-nitrobenzoic acid; ΔΨm, mitochondrial membrane potential

* Corresponding author. Tel.: +55 51 3308 5551; fax: +55 51 3308 5540.
E-mail address: guilhian@ufrgs.br (G. Leipnitz).

http://dx.doi.org/10.1016/j.bbadis.2014.04.022
0925-4439/

Although brain abnormalities are predominant features in patients affected by SO deficiency, the biochemical basis of the pathogenesis characteristic of this disorder is still unclear. Nevertheless, there are evidences that accumulation of sulfite and its derivatives induces oxidative stress [10,11] and disturbs mitochondrial function [12,13] in rat brain, which may contribute for the clinical findings observed in affected patients.

Calcium homeostasis dysregulation has been suggested to play an important role in the pathophysiology of neurodegenerative disorders that are associated with excitotoxicity, bioenergetic dysfunction and oxidative stress [14–16]. Under such pathological conditions, excessive Ca^{2+} uptake by the mitochondrion directly results in organelle dysfunction characterized by exacerbated reactive oxygen species formation, dissipation of the membrane potential, altered redox potential and opening of the mitochondrial permeability transition (MPT) pore, which may lead to cell death [17,18].

Since the effects of sulfite and thiosulfate on mitochondrial function are not totally elucidated, we examined the *in vitro* effects of these compounds on ADP-stimulated state (state 3), resting state (state 4) and carbonyl cyanide m-chlorophenyl hydrazine (CCCP)-stimulated state (uncoupled state) of mitochondrial respiration, the respiratory control ratio (RCR), as well as the activities of glutamate, malate and α-ketoglutarate dehydrogenases in brain mitochondrial preparations from young rats. Considering that a mitochondrial dysfunction can compromise Ca^{2+} buffering system and that this may be involved in the pathogenesis of SO deficiency, we also investigated the influence of sulfite in the presence of micromolar concentrations of Ca^{2+} on mitochondrial membrane potential, swelling, Ca^{2+} retention capacity, matrix NAD(P)H content, membrane protein thiol group content and cytochrome *c* release. We further tested the effect of sulfite on cell viability in cerebral cortex slices.

2. Material and methods

2.1. Reagents

All chemicals, including sodium sulfite, sodium thiosulfate, glutamic acid and malic acid, were purchased from Sigma (St. Louis, MO, USA), except for calcium green-5N that was obtained from Molecular Probes, Invitrogen (Carlsbad, CA), and mouse anti-cytochrome *c* monoclonal antibody and anti-mouse IgG peroxidase-linked antibody from Abcam (Cambridge, UK). Sulfite and thiosulfate were dissolved in the buffer used for each technique and the pH was adjusted to 7.4 immediately before the experiments. The final concentrations of these metabolites in the incubation medium ranged from 1 to 500 μM.

2.2. Animals

Thirty-day-old male Wistar rats, obtained from the Central Animal House of the Department of Biochemistry, ICBS, Universidade Federal do Rio Grande do Sul, Porto Alegre, RS, Brazil, were used. The animals were maintained on a 12:12 h light/dark cycle (lights on 07:00–19:00 h) in air conditioned constant temperature (22 ± 1 °C) colony room, with free access to water and 20% (w/w) protein commercial chow (SUPRA, Porto Alegre, RS, Brazil). The experimental protocol was approved by the Ethics Committee for Animal Research of the Universidade Federal do Rio Grande do Sul, Porto Alegre, Brazil, and followed the NIH Guide for the Care and Use of Laboratory Animals (NIH publication 85-23, revised 1996). All efforts were made to minimize the number of animals used and their suffering.

2.3. Preparation of mitochondrial fractions

Forebrain and liver mitochondria were isolated from 30-day-old rats as previously described [19] with slight modifications [20]. Animals were killed by decapitation, had their brain and liver rapidly removed and put into ice-cold isolation buffer containing 225 mM mannitol, 75 mM sucrose, 1 mM EGTA, 0.1% bovine serum albumin (BSA; fatty acid free) and 10 mM HEPES, pH 7.2. Regarding to the brain, the cerebellum, pons, medulla and olfactory bulbs were removed and the remaining material was used as the forebrain. Both tissues were cut into small pieces using surgical scissors, extensively washed to remove blood and homogenized 1:10 in a Dounce homogenizer using both a loose-fitting and a tight-fitting pestle. The homogenate was centrifuged for 3 min at 2000 *g*. After centrifugation, the supernatant was again centrifuged for 8 min at 12,000 *g*. The pellet was suspended in isolation buffer containing 10 μL of 10% digitonin and centrifuged for 8 min at 12,000 *g*. The final pellet containing the mitochondria was gently washed and suspended in isolation buffer devoid of EGTA, at an approximate protein concentration of 20 $mg \cdot mL^{-1}$. For the measurement of malate dehydrogenase (MDH), glutamate dehydrogenase (GDH) and α-ketoglutarate dehydrogenase (α-KGDH) activities, mitochondrial preparations were submitted to a pre-incubation at 37 °C for 30 min in the absence or presence of sulfite. All experiments were performed in mitochondria with high RCR values, guarantying the full integrity of the preparations.

We carried out parallel experiments with various blanks (controls) in the presence or absence of sulfite and thiosulfate, and also with or without mitochondrial preparations in the incubation medium in order to detect any interference (artifacts) in the techniques utilized to measure the mitochondrial parameters.

2.4. Determination of mitochondrial respiratory parameters by oxygen consumption

Oxygen consumption rate was measured according to Amaral et al. [21] using a Clark-type electrode in a thermostatically controlled (37 °C) and magnetically stirred incubation chamber using glutamate plus malate (2.5 mM each), succinate (5 mM) plus rotenone (2 $\mu g \cdot mL^{-1}$), α-ketoglutarate (5 mM) or pyruvate plus malate (2.5 mM each) as substrates. Sulfite or thiosulfate was added to the reaction medium consisted of 0.3 M sucrose, 5 mM MOPS, 5 mM potassium phosphate, 1 mM EGTA and 0.1% BSA, pH 7.4, and mitochondrial preparations (0.75 mg protein $\cdot mL^{-1}$ using glutamate plus malate, α-ketoglutarate or pyruvate plus malate and 0.5 mg protein $\cdot mL^{-1}$ using succinate). State 3 respiration was measured after the addition of 1 mM ADP to the incubation medium. In order to measure resting (state 4) respiration, 1 $\mu g \cdot mL^{-1}$ oligomycin A was added to the incubation medium. The respiratory control ratio (RCR: state 3/state 4) was then calculated. The uncoupled state was induced by the addition of the classical uncoupler CCCP (1 μM). States 3, 4 and CCCP-induced state were calculated as nmol O_2 consumed $\cdot min^{-1} \cdot$ mg $protein^{-1}$ and the results were expressed as percentage of control.

2.5. Determination of glutamate dehydrogenase (GDH) activity

GDH activity was assayed according to Colon et al. [22]. The reaction mixture contained mitochondrial preparations (60 μg protein $\cdot mL^{-1}$), 50 mM triethanolamine buffer, pH 7.8, 2.6 mM EDTA, 105 mM ammonium acetate, 0.2 mM NADH, 10 mM α-ketoglutarate and 1.0 mM ADP. The reduction of NADH absorbance was monitored spectrophotometrically at 340 nm. GDH activity was calculated as μmol NADH $\cdot min^{-1} \cdot$ mg $protein^{-1}$ and expressed as percentage of control.

2.6. Determination of malate dehydrogenase (MDH) activity

MDH activity was measured according to Kitto [23]. The incubation medium consisted of mitochondrial preparations (7 μg protein $\cdot mL^{-1}$), 10 μM rotenone, 0.1% Triton X-100, 0.14 mM NADH, 0.3 mM oxaloacetate and 50 mM potassium phosphate, pH 7.4. MDH activity was determined following the reduction of NADH fluorescence at wavelengths of excitation and emission of 366 and 450 nm, respectively. MDH activity

was calculated as μmol NADH·min^{-1}·mg protein^{-1} and expressed as percentage of control.

2.7. Determination of α-ketoglutarate dehydrogenase (α-KGDH) complex activity

The activity of α-KGDH complex was evaluated according to Lai and Cooper [24] and Tretter and Adam-Vizi [25] with some modifications. The incubation medium contained mitochondrial preparations (0.25 mg protein·mL^{-1}), 1 mM $MgCl_2$, 0.2 mM thiamine pyrophosphate, 0.4 mM ADP, 10 μM rotenone, 0.2 mM EGTA, 0.12 mM coenzyme A-SH, 1 mM α-ketoglutarate, 2 mM NAD^+, 0.1% Triton X-100 and 50 mM potassium phosphate, pH 7.4. The reduction of NAD^+ was recorded at wavelengths of excitation and emission of 366 and 450 nm, respectively. α-KGDH activity was calculated as nmol NADH·min^{-1}·mg protein^{-1} and expressed as percentage of control.

2.8. Determination of mitochondrial membrane potential (ΔΨm)

The ΔΨm was estimated according to Akerman and Wikstrom [26] and Figueira et al. [27], following the fluorescence of the cationic dye Safranin O (5 μM) on a Hitachi F-4500 spectrofluorometer with magnetic stirring at an excitation and emission of 495 and 586 nm, respectively, using 2.5 mM glutamate plus 2.5 mM malate as substrates. Mitochondrial preparations (0.5 mg protein·mL^{-1}) were incubated at 37 °C with sulfite in 5 mM HEPES buffer, pH 7.2, containing 150 mM potassium chloride, 5 mM magnesium chloride, 0.015 mM EGTA, 5 mM potassium phosphate, 0.01% BSA and 1 μg·mL^{-1} oligomycin A. $CaCl_2$ (10–30 μM) was added to the reaction medium 50 s after the beginning of the assay. In some experiments, the mitochondrial preparations were incubated with cyclosporin A (CsA; 1 μM), ADP (300 μM) or ruthenium red (RR; 1 μM). In the end of each measurement, maximal depolarization was induced by 1 μM carbonyl cyanide-4-(trifluoromethoxy) phenylhydrazone (FCCP). The results are shown as traces representing fluorescence arbitrary units (FAU).

2.9. Determination of mitochondrial swelling

Mitochondrial swelling was assessed by measuring light scattering changes on a Hitachi F-4500 spectrofluorometer with magnetic stirring operating at excitation and emission of 540 nm, using 2.5 mM glutamate plus 2.5 mM malate as substrates. Mitochondrial preparations (0.5 mg protein·mL^{-1}) were incubated at 37 °C with 500 μM sulfite in 5 mM HEPES buffer, pH 7.2, containing 150 mM potassium chloride, 5 mM magnesium chloride, 0.015 mM EGTA, 5 mM potassium phosphate, 0.01% BSA and 1 μg·mL^{-1} oligomycin A. $CaCl_2$ (40 μM) was added to the reaction medium 50 s after the beginning of the assay. In some experiments the mitochondrial preparations were incubated with CsA (1 μM), ADP (300 μM), RR (1 μM), N-acetylcysteine (NAC; 1 mM), catalase (CAT; 500 U·mL^{-1}), melatonin (MEL; 1 mM), coenzyme Q_{10} (CoQ; 50 μM), trifluoperazine (TFZ; 20 μM), chlorpromazine (CP; 20 μM), quinacrine (QUIN; 200 μM), dithiothreitol (DTT; 3 mM) or N-ethylmaleimide (NEM; 20 μM). In the end of each measurement, maximal swelling was induced by the addition of alamethicin (40 μg·mL^{-1}), a pore-forming compound. The results are shown as traces representing FAU.

2.10. Mitochondrial Ca^{2+} retention capacity

Ca^{2+} retention capacity was determined in mitochondria incubated at 37 °C with 500 μM sulfite in 5 mM HEPES buffer, pH 7.2, containing 150 mM potassium chloride, 5 mM magnesium chloride, 0.015 mM EGTA, 5 mM potassium phosphate, 0.01% BSA, 30 μM ADP, 1 μg·mL^{-1} oligomycin A, 2.5 mM glutamate and 2.5 mM malate, and supplemented with 0.2 μM calcium green-5N. A low concentration of ADP (30 μM) was present in the incubation medium to achieve more consistent mitochondrial Ca^{2+} uptake responses [28]. Levels of external free Ca^{2+} were measured by recording the fluorescence of calcium green-5N on a temperature-controlled Hitachi F-4500 spectrofluorometer with magnetic stirring operating at excitation and emission wavelengths of 506 and 532 nm, respectively, and slit width of 5 nm. Two minutes after the addition of mitochondria (0.5 mg·mL^{-1}) to the cuvette, 20 μM $CaCl_2$ was added. In some experiments, the mitochondrial preparations were incubated with CsA (1 μM) and ADP (300 μM). The results are shown as traces representing FAU.

2.11. Determination of NAD(P)H fluorescence

Mitochondrial matrix NAD(P)H autofluorescence was measured at 37 °C on a Hitachi F-4500 spectrofluorometer with magnetic stirring operating at an excitation wavelength of 366 nm and emission wavelength of 450 nm, using 2.5 mM glutamate plus 2.5 mM malate as substrates. Mitochondrial preparations (0.5 mg protein·mL^{-1}) were incubated at 37 °C with 500 μM sulfite in 5 mM HEPES buffer, pH 7.2, containing 150 mM potassium chloride, 5 mM magnesium chloride, 0.015 mM EGTA, 5 mM potassium phosphate, 0.01% BSA and 1 μg·mL^{-1} oligomycin A. $CaCl_2$ (20 μM) was added to the reaction medium 50 s after the beginning of the assay. In some experiments, the mitochondrial preparations were incubated with CsA (1 μM), ADP (300 μM) or RR (1 μM). In the end of the measurements, maximal NAD(P)H oxidation was induced by 1 μM FCCP. The results are shown as traces representing FAU.

2.12. Determination of mitochondrial membrane protein thiol group content

The mitochondrial membrane protein thiol content in rat brain was measured according to Kowaltowski et al. [29] with slight modifications. After mitochondrial swelling experiments, the medium was centrifuged at 15,000 *g* for 2 min in order to sediment the mitochondria. The resultant pellet was resuspended in 5 mM HEPES buffer, pH 7.2, containing 150 mM potassium chloride, 5 mM magnesium chloride, 0.015 mM EGTA, 5 mM potassium phosphate and 0.01% BSA and submitted to three subsequent freeze-thawing procedures to release matrix proteins. A centrifugation was then carried out during 2 min at 15,000 *g*. The pellet was treated with 200 μL of 6.5% trichloroacetic acid and centrifuged at 15,000 *g* during 2 min in order to precipitate the proteins. This procedure was repeated twice. The final pellet was suspended in 200 μL of a medium containing 0.5 mM EDTA and 0.5 M Tris, pH 8.3. Three hundred and forty micrograms of protein were added to 1 mL of a solution containing 100 μM 5,5′-dithio-bis(2-nitrobenzoic acid), 0.5 mM EDTA and 0.5 M Tris, pH 8.3. Absorption was measured at 412 nm. Thiol group content was calculated as nmol 5-thio-2-nitrobenzoic acid (TNB)·mg protein^{-1} and expressed as percentage of control.

2.13. Cytochrome c immunocontent measurement

After mitochondrial swelling experiments, the medium was centrifuged at 12,000 *g* for 10 min in order to sediment the mitochondria. The resultant pellet was resuspended in 1 × RIPA buffer and centrifuged (10,000 *g* for 5 min at 4 °C). Equal amounts of protein (30 μg per well) for each sample prepared in Laemmli-sample buffer (62.5 mM Tris–HCl, pH 6.8, 1% (w/v) SDS, 10% (v/v) glycerol) were fractionated by SDS-PAGE and electro-blotted onto nitrocellulose membranes with Trans-Blot® SD Semi-Dry Electrophoretic Transfer Cell, Bio-Rad (Hercules, CA, USA). Protein loading and electro-blotting efficiency were verified through Ponceau S staining, and the membrane was washed with Tween–Tris buffered saline (Tris 100 mM, pH 7.5, 0.9% NaCl and 0.1% Tween-20). Membranes were incubated for 20 min at room temperature in SNAP i.d.® 2.0 Protein Detection System Merck Millipore (Billerica, MA, USA) with cytochrome *c* primary antibody (1:500 dilution range) and washed with TTBS afterwards. Anti-mouse IgG peroxidase-linked

secondary antibody was incubated with membrane for additional 20 min in SNAP (1:5000 dilution range), washed again and the immunoreactivity was detected by enhanced chemiluminescence using Supersignal West Pico Chemiluminescent kit from Thermo Scientific (Luminol/Enhancer and Stable Peroxide Buffer). Densitometric analysis of the films was performed with Image J software. Blots were developed to be linear in the range used for densitometry. The results were expressed as percentage of control.

2.14. Brain slice preparation

Animals were killed by decapitation and their brains were removed. Four hundred micrometers wide cerebral cortex slices were obtained by using a McIlwain tissue chopper. The slices were washed with 500 μL Hanks' balanced salt solution (HBSS) containing 137 mM NaCl, 0.63 mM Na_2HPO_4, 4.17 mM $NaHCO_3$, 5.36 mM KCl, 0.44 mM KH_2PO_4, 0.41 mM $MgSO_4$, 5.55 mM glucose, 0.49 mM $MgCl_2$ and 1.26 mM $CaCl_2$ and pre-incubated at 37 °C for 3 h with sulfite at the presence of 5% CO_2. The pH was maintained at 7.4.

2.15. MTT reduction

Cell viability was determined in cerebral cortex slices by measuring the reduction of 3-(4,5-dimethylthiazol-2-yl)-2,5-diphenyltetrazolium bromide (MTT) to a dark violet formazan product [30]. After pre-incubation, the slices were washed twice with 500 μL HBSS. MTT reduction assay was performed in plates containing 300 μL HBSS and the reaction was started with the addition of 0.5 $mg \cdot mL^{-1}$ MTT. After 45 min incubation at 37 °C the medium was removed and the slices dissolved in dimethyl sulphoxide. The rate of MTT reduction was measured spectrophotometrically at a wavelength of 570 nm and a reference wavelength of 630 nm. Results were compared to control samples to which 100% viability was attributed.

2.16. Protein determination

Protein content was measured by the method of Bradford [31], using bovine serum albumin as a standard.

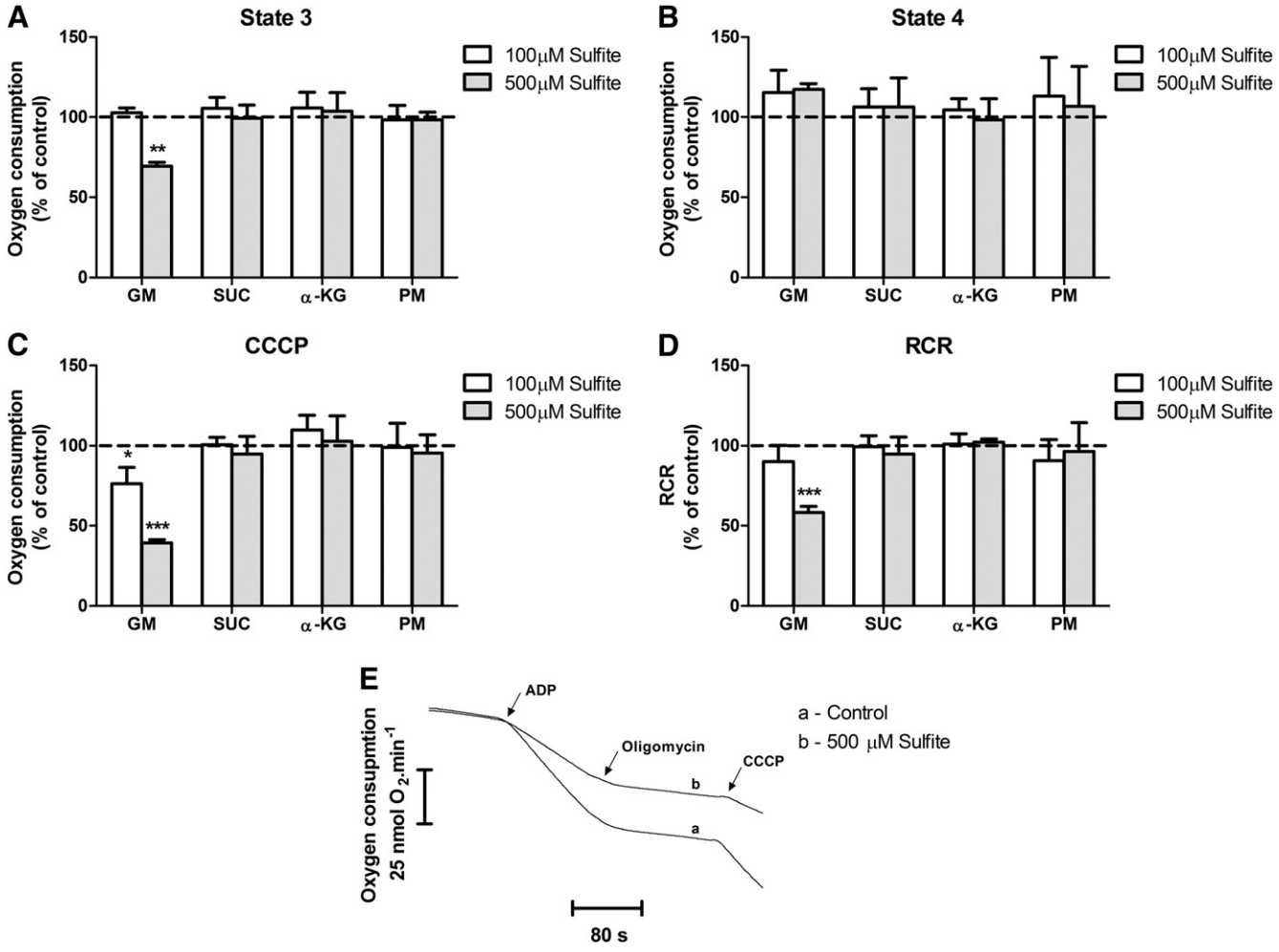

Fig. 1. Effect of sulfite on (A) ADP-stimulated respiration (state 3), (B) resting respiration (state 4), (C) CCCP-stimulated respiration (uncoupled state) and (D) respiratory control ratio (RCR) using brain mitochondria supported by glutamate plus malate (GM), succinate (SUC), α-ketoglutarate (α-KG) and pyruvate plus malate (PM). Sulfite (100 or 500 μM) was added at the beginning of incubation to the reaction medium containing the mitochondrial preparations (0.75 mg protein·mL^{-1} using GM, α-KG or PM and 0.5 mg protein·mL^{-1} using SUC). (E) Representative curve of oxygen concentration in the absence (trace a) or presence of sulfite (500 μM) (trace b) using brain mitochondria supported by GM. The arrows indicate the addition of ADP, oligomycin and CCCP. The slopes of the curve during states 3 and 4 were used for direct calculation of RCR. Values are means ± standard deviation for three to four independent experiments (animals) and are expressed as percentage of controls (Controls: (A) State 3 [nmol $O_2 \cdot min^{-1} \cdot mg$ of $protein^{-1}$]: GM: 80.7 ± 12.7; SUC: 72.2 ± 6.45; α-KG: 41.4 ± 6.54; PM: 124 ± 12.5; (B) State 4 [nmol $O_2 \cdot min^{-1} \cdot mg$ of $protein^{-1}$]: GM: 8.43 ± 1.54; SUC: 13.5 ± 0.87; α-KG: 11.6 ± 0.99; PM: 9.09 ± 0.50; (C) CCCP [nmol $O_2 \cdot min^{-1} \cdot mg$ of $protein^{-1}$]: GM: 85.9 ± 13.9; SUC: 67.0 ± 6.46; α-KG: 27.5 ± 2.59; PM: 124 ± 35.2; (D) RCR: GM: 9.67 ± 0.98; SUC: 5.32 ± 0.19; α-KG: 3.56 ± 0.31; PM: 13.7 ± 2.12). *P < 0.05, ** P < 0.01, *** P < 0.001, compared to controls (Duncan multiple range test).

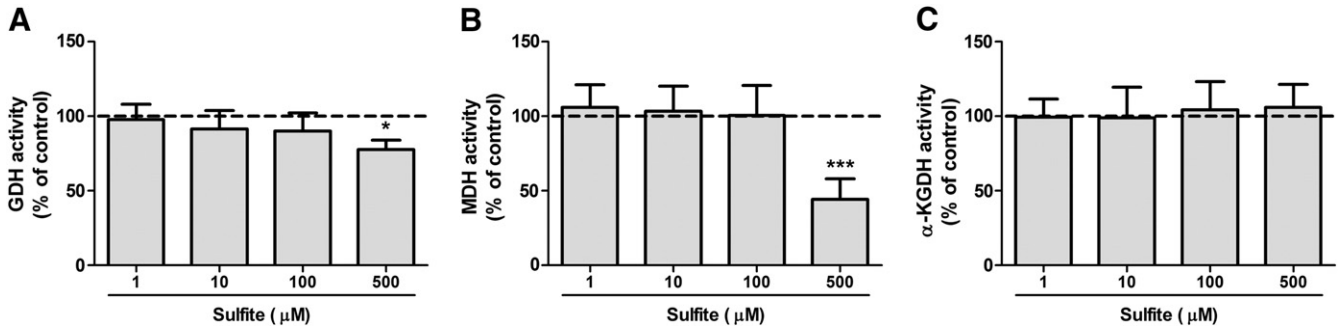

Fig. 2. Effect of sulfite on (A) glutamate dehydrogenase (GDH), (B) malate dehydrogenase (MDH) and (C) α-ketoglutarate dehydrogenase (α-KGDH) activities in brain mitochondria. Sulfite (1–500 μM) was added to the reaction medium containing the mitochondrial preparations and incubated for 30 min. Values are means ± standard deviation for four to six independent experiments (animals) and are expressed as percentage of controls. (Controls: (A) GDH [μmol NADH·min^{-1}·mg protein^{-1}]: 74.49 ± 4.470; (B) MDH [μmol NADH·min^{-1}·mg protein^{-1}]: 6377 ± 570.5; (C) α-KGDH [nmol NADH·min^{-1}·mg protein^{-1}]: 54.17 ± 11.04). *P < 0.05, *** P < 0.001, compared to controls (Duncan multiple range test).

2.17. Statistical analysis

Results are presented as mean ± standard deviation. Assays were performed in duplicate or triplicate and the mean was used for statistical analysis. Data were analyzed by one-way ANOVA, followed by the post hoc Duncan multiple range test when F was significant. Only significant F values are shown in the text. Differences between groups were rated significant at $P < 0.05$. All analyses were carried out using the Statistical Package for the Social Sciences (SPSS) software.

3. Results

3.1. Sulfite alters oxygen consumption in brain mitochondria supported by glutamate plus malate

First, we determined the effect of sulfite and thiosulfate on brain mitochondrial oxygen consumption using glutamate plus malate, succinate, α-ketoglutarate or pyruvate plus malate as substrates. Fig. 1 shows that brain mitochondria incubated under our experimental conditions were well functioning, as indicated by the higher respiratory rates observed in the presence of ADP (state 3) relatively to those obtained after the addition of the ATP synthase inhibitor oligomycin A (state 4). It was verified that sulfite decreased state 3 respiration [$F_{(2,9)} = 15.546$, $P < 0.01$] (Fig. 1A), CCCP-induced state respiration (uncoupled state) [$F_{(2,9)} = 30.413$, $P < 0.001$] (Fig. 1C) and RCR [$F_{(2,9)} = 25.149$, $P < 0.001$] (Fig. 1D), but not state 4 (Fig. 1B), in mitochondria supported by glutamate plus malate. In contrast, sulfite did not alter mitochondrial respiration when succinate, α-ketoglutarate or pyruvate plus malate were used as substrates. Moreover, thiosulfate did not affect mitochondrial oxygen consumption regardless of the substrate used (results not shown). Fig. 1E shows a representative respiration curve demonstrating the transition from state 3 to state 4. This figure allows a direct calculation of state 3, state 4 and RCR.

3.2. Sulfite inhibits GDH and MDH activities in brain mitochondria

We assessed the effect of sulfite on the activities of GDH, MDH and α-KGDH in mitochondrial preparations in order to evaluate whether the inhibition of brain mitochondrial respiration caused by this metabolite in the presence of glutamate plus malate as substrates could be explained by the impairment of glutamate and malate oxidation. Figs. 2A and B show that sulfite inhibited GDH [$F_{(4,15)} = 3.163$, $P < 0.05$] and MDH [$F_{(4,25)} = 17.192$, $P < 0.001$] activities. In contrast, α-KGDH activity was not altered by sulfite (Fig. 2C).

Since MDH was more vulnerable than GDH to sulfite effects, we evaluated the influence of this metabolite on the activity of a commercial solution of MDH. It can be observed that sulfite inhibited the activity of purified MDH and that the antioxidants catalase (CAT) and melatonin (MEL), as well as the reductant agent DTT attenuated this effect [$F_{(4,18)} = 38.711$, $P < 0.001$] (Fig. 3). Our results showing that antioxidants and DTT partially prevented this effect suggest that reactive species and modification of thiol groups on the enzyme, respectively, are involved in the inhibition of MDH activity.

3.3. Sulfite induces mitochondrial membrane potential (ΔΨm) dissipation and swelling in the presence of Ca^{2+} in brain mitochondria supported by glutamate plus malate

The next set of experiments was carried out to investigate the effect of sulfite on ΔΨm in state 4 respiring mitochondria in the absence or presence of Ca^{2+} (10–30 μM), using glutamate plus malate as substrates. It can be seen in Fig. 4A that sulfite caused a progressive reduction of ΔΨm after the addition of increasing Ca^{2+} concentrations. In contrast, no effect could be observed in the absence of Ca^{2+} in the incubation medium. We then evaluated the effect of raising sulfite concentrations (10–500 μM) on ΔΨm in the presence of Ca^{2+} (20 μM) and observed that sulfite dissipates ΔΨm in a dose-dependent manner (Fig. 4B). RR, a potent inhibitor of the mitochondrial Ca^{2+} uptake, was able to prevent sulfite-induced ΔΨm reduction, implying that sulfite effects are dependent on the entrance of Ca^{2+} into the mitochondria. Furthermore, the decrease of ΔΨm provoked by sulfite in the presence of Ca^{2+} was prevented by CsA and ADP, inhibitors of MPT (Fig. 4C).

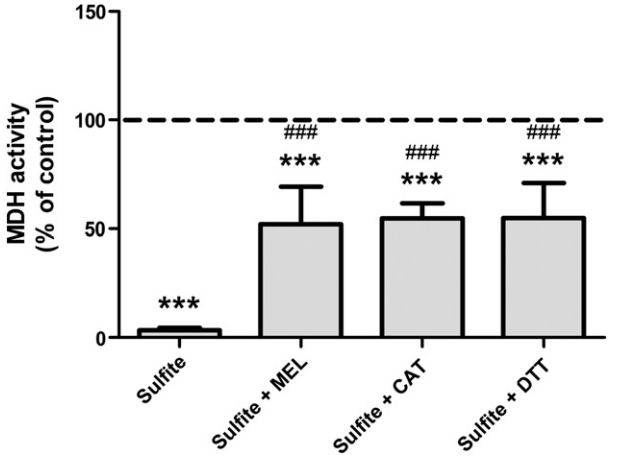

Fig. 3. Effect of sulfite on the activity of a commercial solution of malate dehydrogenase (MDH). Sulfite (500 μM) was added do the reaction medium containing purified MDH and incubated for 30 min. In some experiments, melatonin (MEL; 1500 μM), catalase (CAT; 500 U·mL^{-1}) or dithiothreitol (DTT; 5 mM) was co-incubated with 500 μM sulfite. Values are means ± standard deviation for three to five independent experiments (animals) and are expressed as percentage of controls. (Control: MDH [mmol NADH·min^{-1}·mg protein^{-1}]: 3822 ± 506.1). *** P < 0.001, compared to control; ###P < 0.001, compared to sulfite (Duncan multiple range test).

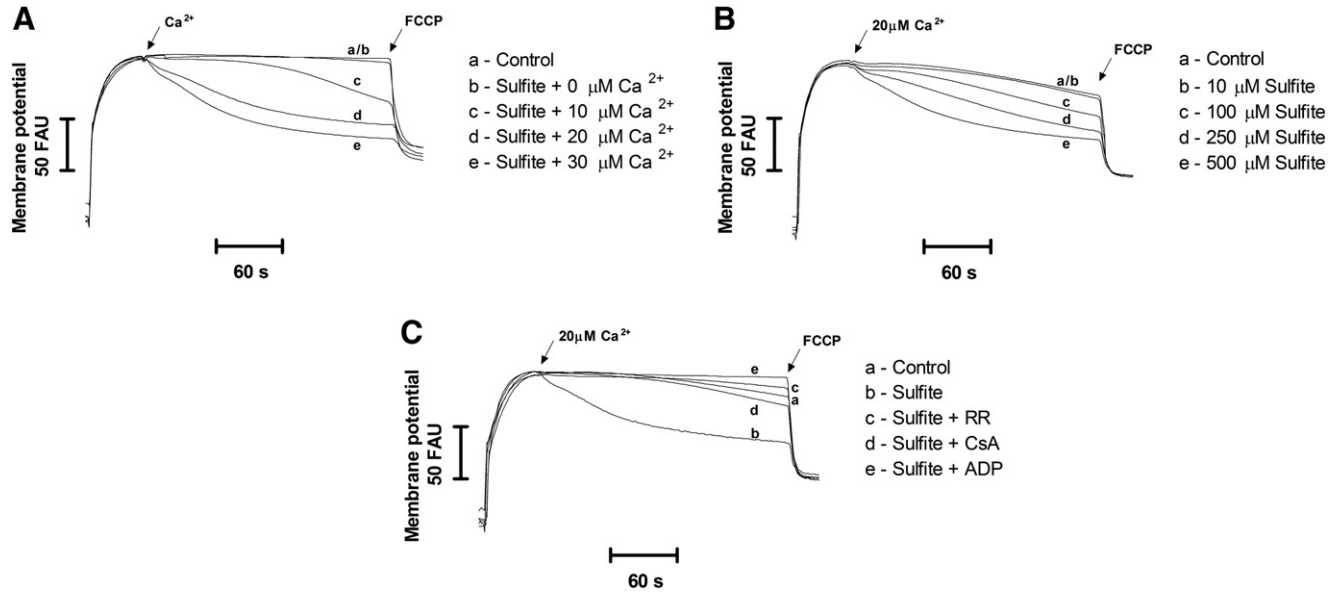

Fig. 4. Effect of sulfite on mitochondrial membrane potential (ΔΨm) using brain mitochondria supported by glutamate plus malate in the absence or presence of Ca^{2+}. (A) Sulfite (500 μM) (trace b) was added at the beginning of incubation to the reaction medium containing the mitochondrial preparations (0.5 mg protein·mL^{-1}). Increasing concentrations of Ca^{2+} (0 μM, trace b; 10 μM, trace c; 20 μM, trace d; 30 μM, trace e) were added 50 s afterwards. (B) Increasing concentrations of sulfite (10 μM, trace b; 100 μM, trace c; 250 μM, trace d; 500 μM, trace e) were added at the beginning of incubation to the reaction medium containing the mitochondrial preparations (0.5 mg protein·mL^{-1}). Ca^{2+} (20 μM) was added 50 s afterwards. (C) Sulfite (500 μM) (trace b) was added at the beginning of incubation to the reaction medium containing the mitochondrial preparations (0.5 mg protein·mL^{-1}). Ca^{2+} (20 μM) was added 50 s afterwards. In some experiments, the mitochondrial preparations were incubated with sulfite plus ruthenium red (RR; 1 μM; trace c), cyclosporine A (CsA; 1 μM; trace d) or ADP (300 μM; trace e). Control (trace a) in graphic A was performed in the absence of Ca^{2+} and sulfite, whereas controls (traces a) in graphics B and C were performed in the presence of Ca^{2+} (20 μM) and did not contain sulfite. FCCP (1 μM) was added at the end of the experiment, as indicated. Traces are representative of three independent experiments and express fluorescence arbitrary units (FAU).

In order to further study a possible involvement of the non-selective inner membrane permeabilization due to MPT pore opening with sulfite-induced ΔΨm decrease, we measured mitochondrial swelling by following light scattering changes. It was verified that sulfite caused swelling in the presence of Ca^{2+} in brain mitochondria and that this effect was fully prevented by RR, CsA and ADP, reinforcing therefore the induction of MPT by sulfite (Fig. 5A). In contrast, sulfite did not induce swelling in mitochondrial preparations from rat liver, implying that brain is more vulnerable to the toxic effects of this metabolite (Fig. 5B).

3.4. Sulfite reduces Ca^{2+} retention capacity in brain mitochondria supported by glutamate plus malate

We then investigated the influence of sulfite on mitochondrial Ca^{2+} retention, since MPT induction leads to a rapid release of Ca^{2+} from mitochondria. As shown in Fig. 6, sulfite reduced the mitochondrial Ca^{2+} retention capacity compared with control mitochondria supported by glutamate plus malate. Furthermore, CsA and ADP prevented this effect, indicating the involvement of MPT induction in the mitochondrial Ca^{+2} handling disruption induced by sulfite.

3.5. Sulfite decreases mitochondrial matrix NAD(P)H pool in the presence of Ca^{2+} in brain mitochondria supported by glutamate plus malate

Sulfite reduced NAD(P)H fluorescence in the presence of Ca^{2+} in mitochondria supported by glutamate plus malate (Fig. 7), suggesting that this metabolite decreased NAD(P)H pool due either to a oxidation of the reduced equivalents or their loss from the matrix. CsA, ADP and RR were able to prevent this effect, suggesting the involvement of MPT induction.

3.6. NEM prevents sulfite-induced swelling in the presence of Ca^{2+} in brain mitochondria supported by glutamate plus malate

In the next step, we evaluated whether compounds reported to inhibit the MPT, such as phospholipase A2 inhibitors (TFZ, CP and QUIN)

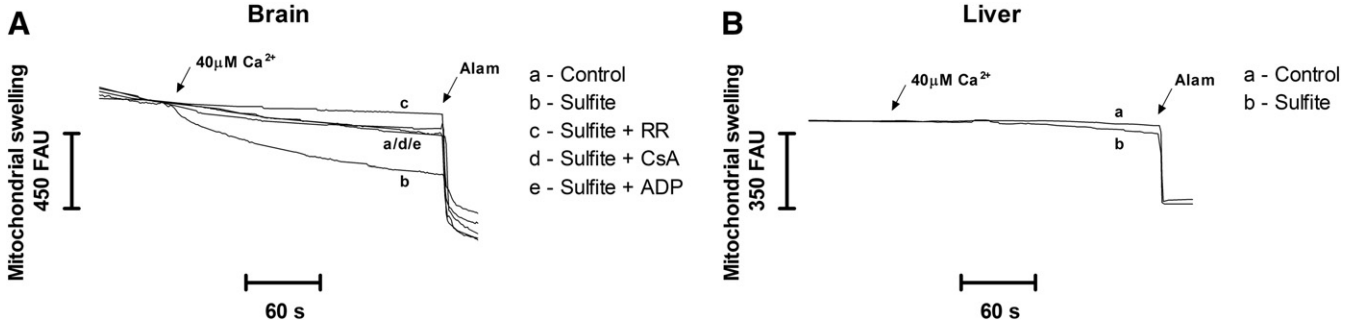

Fig. 5. Effect of sulfite on mitochondrial swelling using (A) brain or (B) liver mitochondria supported by glutamate plus malate in the presence of Ca^{2+}. Sulfite (500 μM) (trace b) was added at the beginning of incubation to the reaction medium containing the mitochondrial preparations (0.5 mg protein·mL^{-1}). Ca^{2+} (40 μM) was added 50 s afterwards. In some experiments, the mitochondrial preparations were incubated with sulfite plus ruthenium red (RR; 1 μM; trace c), cyclosporine A (CsA; 1 μM; trace d) or ADP (300 μM; trace e). Controls (traces a) were performed in the presence of Ca^{2+} (40 μM) and did not contain sulfite. Alamethicin (Alam; 40 μg·mg of $protein^{-1}$) was added at the end of the experiment, as indicated. Traces are representative of three independent experiments and express fluorescence arbitrary units (FAU).

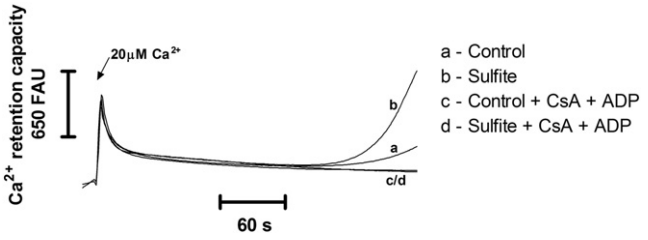

Fig. 6. Effect of sulfite on mitochondrial Ca^{2+} retention capacity using brain mitochondria supported by glutamate plus malate in the presence of Ca^{2+}. Sulfite (500 μM) (trace b) was added at the beginning of incubation to the reaction medium containing ADP (30 μM) and the mitochondrial preparations (0.5 mg protein·mL^{-1}). Ca^{2+} (20 μM) was added afterwards. In some experiments, the mitochondrial preparations were incubated with sulfite and cyclosporine A (CsA; 1 μM) plus ADP (300 μM; trace d). Controls (traces a and c) were performed in the presence of 20 μM Ca^{2+} and did not contain sulfite. Traces are representative of three independent experiments and express fluorescence arbitrary units (FAU).

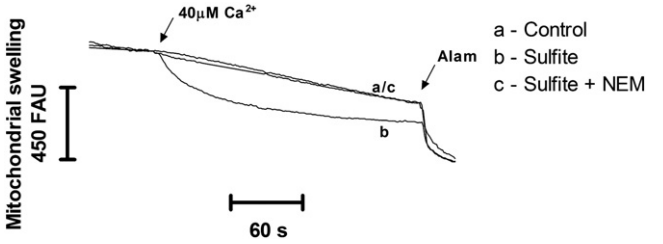

Fig. 8. Effect of N-ethylmaleimide (NEM; 20 μM) on sulfite-induced mitochondrial swelling using brain mitochondria supported by glutamate plus malate in the presence of Ca^{2+}. Sulfite (500 μM) (trace b) was added at the beginning of incubation to the reaction medium containing the mitochondrial preparations (0.5 mg protein·mL^{-1}). Ca^{2+} (40 μM) was added 50 s afterwards. In some experiments, the mitochondrial preparations were incubated with sulfite plus NEM (trace c). Control (trace a) was performed in the presence of Ca^{2+} (40 μM) and did not contain sulfite. Alamethicin (Alam; 40 μg·mg of protein^{-1}) was added at the end of the experiment, as indicated. Traces are representative of three independent experiments and express fluorescence arbitrary units (FAU).

[32,33], antioxidants (NAC, CAT, MEL and CoQ) [34,35], the reductant reagent DTT [29,36,37] and the hydrophobic thiol reagent NEM [29,36–38], could prevent the mitochondrial swelling induced by sulfite. We found that the inhibitors of phospholipase A2, antioxidants and DTT did not alter this effect (results not shown). In contrast, NEM prevented sulfite-induced swelling in the presence of Ca^{2+}, suggesting that sulfite exerts a direct effect on thiol groups of proteins involved in MPT pore formation (Fig. 8).

3.7. Sulfite decreases the content of thiol groups in the presence of Ca^{2+} in brain mitochondria supported by glutamate plus malate

Our results also demonstrate that 500 μM sulfite significantly decreased the content of thiol groups in the presence of Ca^{2+} in brain mitochondria [$F_{(2,11)} = 34.591$, $P < 0.001$] (Fig. 9), reinforcing the view that sulfite has a direct effect on these groups. We further observed that 200 μM NEM decreased this parameter in the same conditions (positive control) (Fig. 9).

3.8. Sulfite induces cytochrome c release from brain mitochondria in the presence of Ca^{2+}

We measured the effect of sulfite on cytochrome *c* release from mitochondria. We found that sulfite markedly decreased mitochondrial cytochrome *c* immunocontent [$F_{(2,6)} = 119.171$, $P < 0.001$] (Fig. 10), indicating an increase of cytochrome *c* release from the mitochondria. CsA attenuated this effect, implying that it occurred due to sulfite-induced MPT in the presence of Ca^{2+}.

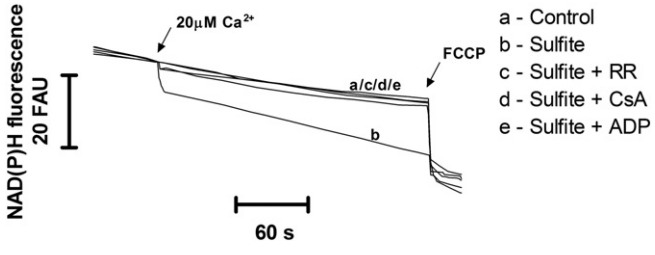

Fig. 7. Effect of sulfite on mitochondrial NAD(P)H content using brain mitochondria supported by glutamate plus malate in the presence of Ca^{2+}. Sulfite (500 μM) (trace b) was added at the beginning of incubation to the reaction medium containing the mitochondrial preparations (0.5 mg protein·mL^{-1}). Ca^{2+} (20 μM) was added 50 s afterwards. In some experiments, the mitochondrial preparations were incubated with sulfite plus ruthenium red (RR; 1 μM; trace c), cyclosporine A (CsA; 1 μM; trace d) or ADP (300 μM; trace e). Control (trace a) was performed in the presence of Ca^{2+} (20 μM) and did not contain sulfite. FCCP (1 μM) was added at the end of the experiment, as indicated. Traces are representative of three independent experiments and express fluorescence arbitrary units (FAU).

3.9. Sulfite reduces cell viability in cerebral cortex slices

We finally examined the effect of sulfite on cell viability in cerebral cortex slices through MTT reduction in order to check whether sulfite could induce injury to intact cells. We found that sulfite significantly decreased MTT reduction and that CsA prevented this effect [$F_{(2,10)} = 6.566$, $P < 0.05$] (Fig. 11), implying that sulfite-mediated MPT pore opening causes cell injury.

4. Discussion

High tissue levels of sulfite and thiosulfate are characteristic of isolated SO deficiency and molybdenum cofactor deficiency. Affected patients predominantly present neonatal seizures, encephalopathy and psychomotor retardation, whose pathophysiology is uncertain. However, some evidences indicate that mitochondrial dysfunction caused by the accumulating metabolites may be involved in the neurological dysfunction of these diseases [2,7,12,13,39]. In this particular, it should be emphasized that lactic acidemia has been described in affected patients [2,7,39]. Therefore, in the present study we investigated the effect of sulfite and thiosulfate on brain mitochondrial homeostasis.

We first verified that sulfite, but not thiosulfate, decreased oxygen consumption in state 3 and uncoupled respiration in mitochondria supported by glutamate plus malate, that are electron donors of complex I, but not with succinate, which donates electrons to complex II, and other NADH-linked substrates (α-ketoglutarate or pyruvate plus malate). Our

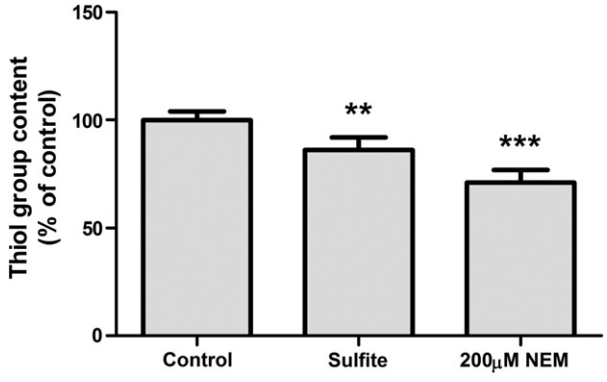

Fig. 9. Effect of sulfite on thiol group content in brain mitochondria supported by glutamate plus malate in the presence of Ca^{2+}. Sulfite (500 μM) and Ca^{2+} (40 μM) were added to the incubation medium containing the mitochondrial preparations (0.5 mg protein·mL^{-1}). In some experiments, the mitochondrial preparations were incubated with N-ethylmaleimide (NEM; 200 μM). Values are means ± standard deviation for four to five independent experiments (animals) and are expressed as percentage of control (Control: 54.0 ± 2.13 nmol TNB·mg protein^{-1}). ** $P < 0.01$, *** $P < 0.001$, compared to control (Duncan multiple range test).

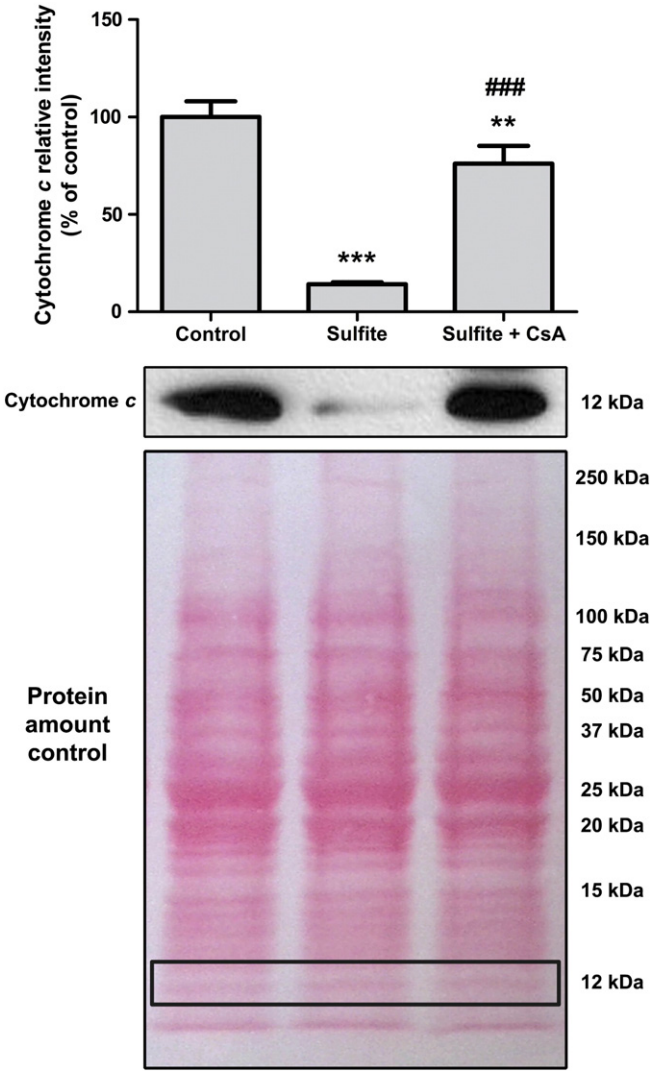

Fig. 10. Effect of sulfite on cytochrome *c* immunocontent in brain mitochondria supported by glutamate plus malate in the presence of Ca^{2+}. Sulfite (500 μM) and Ca^{2+} (40 μM) were added to the incubation medium containing the mitochondrial preparations (0.5 mg protein·mL^{-1}). In some experiments, the mitochondrial preparations were incubated with sulfite plus cyclosporine A (CsA; 1 μM). A representative immunoblot of cytochrome *c* is also displayed. Values are means ± standard deviation for three to four independent experiments (animals) and are expressed as percentage of control (Control: 33091 ± 2660 arbitrary units). **P < 0.01, *** P < 0.001, compared to control; ###P < 0.001, compared to sulfite (Duncan multiple range test).

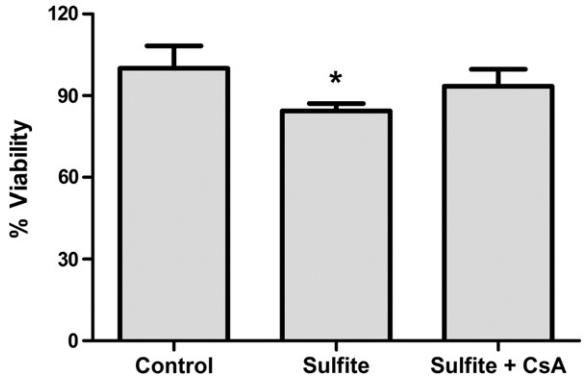

Fig. 11. Effect of sulfite on cerebral cortex slices viability determined by MTT reduction assay. Rat cerebral cortex slices were incubated for 3 h in the absence or presence of 500 μM sulfite and 1 μM cyclosporine (CsA). Values are mean ± standard deviation for three to four independent experiments (animals) and are expressed as percentage of control. *P < 0.05, compared to control (Duncan multiple range test).

findings are in accordance with the results found by Zhang and collaborators [12], showing that sulfite causes ATP depletion in PC12 and Neuro-2a cells. Taken together, these data indicate that sulfite-induced decrease of mitochondrial respiration occurred due to a blockage of glutamate and/or malate oxidation. We further verified that sulfite inhibited GDH and MDH activities, whereas no alteration was observed in α-KGDH activity. In the brain, GDH reaction occurs mainly in the direction of oxidative deamination of glutamate forming NADH and α-ketoglutarate, which can be oxidized through the Krebs cycle [40]. MDH, in turn, is a Krebs cycle enzyme and also a component in the malate-aspartate shuttle system. Therefore, it is presumed that the mitochondrial respiration impairment caused by sulfite may be due to the inhibition of glutamate and malate oxidation through GDH and MDH, which causes a decrease in the availability of intermediates of tricarboxylic acid cycle and a lack of reduced equivalents to supply the respiratory chain. These findings are in line with those observed by Zhang and colleagues [12], who showed that 100 μM sulfite, which was the highest dose tested, moderately inhibits MDH activity and markedly diminished GDH activity. We further verified that CAT, MEL and DTT prevented the inhibition of the activity of purified MDH caused by sulfite. So, it may be presumed that reactive species scavenged by MEL and CAT are involved in this effect. The fact that DTT also attenuated this effect suggests that thiol groups on the enzyme are vulnerable to sulfite. However, we cannot ascertain whether the alterations of the enzyme thiol groups are mediated through reactive species or a direct attack of sulfite. It should be also noted that α-aminoadipic semialdehyde (AASA) dehydrogenase is inhibited *in vitro* by sulfite, leading to increased levels of α-AASA and its cyclic form piperideine-6-carboxylate (P6C). In this particular, the increase of α-AASA and P6C due to sulfite accumulation could contribute to the pathophysiology of SO deficiency, since P6C acts as a trapping agent of pyridoxal-5-phosphate [41,42].

Next, we observed that sulfite decreased the ΔΨm and induced swelling in brain mitochondria in the presence of Ca^{2+}, but not in the absence of this cation. In addition, the prevention of these effects by RR, a potent inhibitor of the mitochondrial Ca^{2+} uptake [43], supports the importance of the involvement of Ca^{2+} in these effects. It is well known that mitochondria play a central role in cytosolic Ca^{2+} buffering, although an abnormal increase in mitochondrial Ca^{2+} uptake may induce MPT and lead to apoptosis in different cells [18,44,45]. The MPT causes a non-selective traffic between the mitochondrial matrix and the cytosol, allowing the influx of water and substances up to 1.5 kDa into the matrix and leading to mitochondrial swelling, loss of metabolites (Ca^{2+}, glutathione, NADH and NADPH), ΔΨm collapse, impairment of oxidative phosphorylation and ATP synthesis, as well as release of proapoptotic factors, such as cytochrome *c* [46–48]. On the other hand, sulfite did not provoke swelling in liver mitochondria, which is in accordance with the fact that patients with SO deficiency do not present hepatic dysfunction.

Our results also showed that the decrease of ΔΨm elicited by sulfite is due to a non-selective membrane permeabilization caused by MPT pore opening, since ΔΨm dissipation was accompanied by mitochondrial swelling and was inhibited by CsA and ADP. In this particular, CsA inhibits MPT by binding cyclophilin D, a mitochondrial matrix protein which has been reported to be a MPT pore modulator through its interaction with the adenine nucleotide translocator (ANT) [44,49,50]. Furthermore, it is known that adenine nucleotides inhibit MPT pore through their binding to ANT [18,28]. Our data showing that sulfite reduced the mitochondrial Ca^{2+} retention capacity and that this effect was prevented by CsA plus ADP are also in line with the induction of MPT pore opening by synergistical effects of sulfite and Ca^{2+}.

We further verified that NEM prevented the mitochondrial swelling induced by sulfite in the presence of Ca^{2+}. NEM is an alkylating agent that reacts with sulfhydryl groups to form stable thioether bonds. Previous reports demonstrated that NEM has access to critical thiol groups on ANT that regulate the MPT pore opening [37,51,52]. Therefore, our data showing that NEM prevented the mitochondrial swelling caused by

sulfite indicate that this compound modulates MPT by attacking thiol groups, which increases the probability of pore opening. This is reinforced by our findings showing that sulfite decreased the content of thiol groups in brain mitochondria and is in accordance with other evidences demonstrating that sulfite reacts directly with sulfhydryl groups [1]. On the other hand, since antioxidants did not prevent sulfite-induced swelling, it may be suggested that the reactive species generated from this metabolite do not alter critical groups involved in MPT pore opening. Indeed, it has been reported that other compounds, such as acetoacetate, phenylarsine oxide and 4,4′-diisothiocyanatostilbene-2,2′-disulfonic acid, are able to induce MPT independently of reactive species [29,37,38,51]. It is also of note that Costantini and collaborators [36] reported that at least two distinct sites containing thiol groups modulate MPT and that one site is insensitive to reductants like DTT.

Sulfite also diminished the mitochondrial matrix NAD(P)H levels in the presence of Ca^{2+}. The loss of the mitochondrial pool of pyridine nucleotides could be explained by a release of NAD(P)H from the mitochondria through the MPT pore, which can lead to the impairment of mitochondrial redox homeostasis. In fact, the matrix NAD(P)H pool decrease elicited by sulfite was inhibited by CsA and ADP, implying that this effect was caused by MPT induction.

We also found that sulfite reduced mitochondrial cytochrome *c* immunocontent, which could be related to the MPT induced by this compound. In this regard, the release of cytochrome *c* from the mitochondrial intermembrane space into the cytosol typically accompanies the osmotic swelling and the physical rupture of the mitochondrial outer membrane provoked by MPT [53,54]. The observation that the decrease of mitochondrial cytochrome *c* immunocontent was prevented by CsA supports this hypothesis. The release of cytochrome *c* from mitochondria into the cytosol plays a key role in the apoptosis induction by forming the apoptosome complex with Apaf-1 and procaspase-9 and initiating the caspase cascade [48,55]. Thus, our results suggest that sulfite may induce apoptosis by promoting MPT in the presence of Ca^{2+}. In line with this, we verified that sulfite decreased cell viability in cerebral cortex and that CsA, an inhibitor of MPT pore opening, prevented this effect.

It is noteworthy that neurons are more susceptible to the induction of MPT due to increases in intracellular Ca^{2+} levels after NMDA receptor overstimulation (excitotoxicity). In this context, it should be emphasized that S-sulfocysteine, a metabolite structurally similar to glutamate generated from sulfite and free cysteine, is able to activate NMDA receptors [56,57], leading to high Ca^{2+} influx. Furthermore, the inhibition of GDH by sulfite could lead to high levels of glutamate in the synaptic cleft, contributing to the raise of intracellular Ca^{2+} concentrations. In addition, energy metabolism dysfunction induced by sulfite could also play an important role in Ca^{2+} dyshomeostasis through the impairment of Ca^{2+} removal systems. Therefore, it is hypothesized that a failure in Ca^{2+} handling by the mitochondrion is potentially involved in the neuropathology of SO deficiency.

In conclusion, our study provides for the first time evidence that sulfite acts synergistically with Ca^{2+} inducing MPT in the brain mediated by a direct attack of sulfite on critical protein cysteinyl groups of the transition pore. Therefore, it is presumed that bioenergetic dysfunction and MPT induction may be important pathomechanisms underlying the pathogenesis of the neurological dysfunction observed in SO deficient patients.

Acknowledgements

This work was supported by grants from Conselho Nacional de Desenvolvimento Científico e Tecnológico (CNPq), Programa de Apoio a Núcleos de Excelência (PRONEX II), Fundação de Amparo à Pesquisa do Estado do Rio Grande do Sul (FAPERGS), Pró-Reitoria de Pesquisa/Universidade Federal do Rio Grande do Sul (PROPESQ/UFRGS), Financiadora de estudos e projetos (FINEP), Rede Instituto Brasileiro de Neurociência (IBN-Net) # 01.06.0842-00 and Instituto Nacional de Ciência e Tecnologia em Excitotoxicidade e Neuroproteção (INCT-EN).

References

[1] J.L. Johnson, M. Duran, Molybdenum cofactor deficiency and isolated sulfite oxidase deficiency, in: B.A. Scriver CR, D. Valle, W.S. Sly (Eds.), The Metabolic and Molecular Bases of Inherited Disease, McGraw-Hill, New York, 2001, pp. 3181–3217.
[2] S.N. Basheer, P.J. Waters, C.W. Lam, C. Acquaviva-Bourdain, G. Hendson, K. Poskitt, J. Hukin, Isolated sulfite oxidase deficiency in the newborn: lactic acidaemia and leukoencephalopathy, Neuropediatrics 38 (2007) 38–41.
[3] C. Feng, G. Tollin, J.H. Enemark, Sulfite oxidizing enzymes, Biochim. Biophys. Acta 1774 (2007) 527–539.
[4] S.L. Taylor, N.A. Higley, R.K. Bush, Sulfites in foods: uses, analytical methods, residues, fate, exposure assessment, metabolism, toxicity, and hypersensitivity, Adv. Food Res. 30 (1986) 1–76.
[5] K. Chapman, Sulfite-containing pharmaceuticals, Can. Med. Assoc. J. 148 (1993) 714.
[6] W.H. Tan, F.S. Eichler, S. Hoda, M.S. Lee, H. Baris, C.A. Hanley, P.E. Grant, K.S. Krishnamoorthy, V.E. Shih, Isolated sulfite oxidase deficiency: a case report with a novel mutation and review of the literature, Pediatrics 116 (2005) 757–766.
[7] C.A. Rupar, J. Gillett, B.A. Gordon, D.A. Ramsay, J.L. Johnson, R.M. Garrett, K.V. Rajagopalan, J.H. Jung, G.S. Bacheyie, A.R. Sellers, Isolated sulfite oxidase deficiency, Neuropediatrics 27 (1996) 299–304.
[8] K. Vijayakumar, R. Gunny, S. Grunewald, L. Carr, K.W. Chong, C. DeVile, R. Robinson, N. McSweeney, P. Prabhakar, Clinical neuroimaging features and outcome in molybdenum cofactor deficiency, Pediatr. Neurol. 45 (2011) 246–252.
[9] M.C. Edwards, J.L. Johnson, B. Marriage, T.N. Graf, K.E. Coyne, K.V. Rajagopalan, I.M. MacDonald, Isolated sulfite oxidase deficiency: review of two cases in one family, Ophthalmology 106 (1999) 1957–1961.
[10] F. Chiarani, C.S. Bavaresco, C.S. Dutra-Filho, C.A. Netto, A.T. Wyse, Sulfite increases lipoperoxidation and decreases the activity of catalase in brain of rats, Metab. Brain Dis. 23 (2008) 123–132.
[11] Z. Abedinzadeh, Sulfur-centered reactive intermediates derived from the oxidation of sulfur compounds of biological interest, Can. J. Physiol. Pharmacol. 79 (2001) 166–170.
[12] X. Zhang, A.S. Vincent, B. Halliwell, K.P. Wong, A mechanism of sulfite neurotoxicity: direct inhibition of glutamate dehydrogenase, J. Biol. Chem. 279 (2004) 43035–43045.
[13] M. Grings, A.P. Moura, B. Parmeggiani, G.F. Marcowich, A.U. Amaral, A.T. de Souza Wyse, M. Wajner, G. Leipnitz, Disturbance of brain energy and redox homeostasis provoked by sulfite and thiosulfate: potential pathomechanisms involved in the neuropathology of sulfite oxidase deficiency, Gene 531 (2013) 191–198.
[14] S. Gandhi, A. Wood-Kaczmar, Z. Yao, H. Plun-Favreau, E. Deas, K. Klupsch, J. Downward, D.S. Latchman, S.J. Tabrizi, N.W. Wood, M.R. Duchen, A.Y. Abramov, PINK1-associated Parkinson's disease is caused by neuronal vulnerability to calcium-induced cell death, Mol. Cell 33 (2009) 627–638.
[15] J.T. Yu, R.C. Chang, L. Tan, Calcium dysregulation in Alzheimer's disease: from mechanisms to therapeutic opportunities, Prog. Neurobiol. 89 (2009) 240–255.
[16] T.R. Rosenstock, A.C. Carvalho, A. Jurkiewicz, R. Frussa-Filho, S.S. Smaili, Mitochondrial calcium, oxidative stress and apoptosis in a neurodegenerative disease model induced by 3-nitropropionic acid, J. Neurochem. 88 (2004) 1220–1228.
[17] I.B. Zavodnik, I.K. Dremza, V.T. Cheshchevik, E.A. Lapshina, M. Zamaraewa, Oxidative damage of rat liver mitochondria during exposure to t-butyl hydroperoxide. Role of Ca(2)(+) ions in oxidative processes, Life Sci. 92 (2013) 1110–1117.
[18] M. Crompton, The mitochondrial permeability transition pore and its role in cell death, Biochem. J. 341 (Pt 2) (1999) 233–249.
[19] R.E. Rosenthal, F. Hamud, G. Fiskum, P.J. Varghese, S. Sharpe, Cerebral ischemia and reperfusion — prevention of brain mitochondrial injury by lidoflazine, J. Cereb. Blood Flow Metab. 7 (1987) 752–758.
[20] S.R. Mirandola, D.R. Melo, P.F. Schuck, G.C. Ferreira, M. Wajner, R.F. Castilho, Methylmalonate inhibits succinate-supported oxygen consumption by interfering with mitochondrial succinate uptake, J. Inherit. Metab. Dis. 31 (2008) 44–54.
[21] A.U. Amaral, G. Leipnitz, C.G. Fernandes, B. Seminotti, P.F. Schuck, M. Wajner, Alpha-ketoisocaproic acid and leucine provoke mitochondrial bioenergetic dysfunction in rat brain, Brain Res. 1324 (2010) 75–84.
[22] A.D. Colon, A. Plaitakis, A. Perakis, S. Berl, D.D. Clarke, Purification and characterization of a soluble and a particulate glutamate dehydrogenase from rat brain, J. Neurochem. 46 (1986) 1811–1819.
[23] G.B. Kitto, Intra- and extramitochondrial malate dehydrogenase from chicken and tuna heart, Methods Enzymol. 13 (1969) 106–116.
[24] J.C. Lai, A.J. Cooper, Brain alpha-ketoglutarate dehydrogenase complex: kinetic properties, regional distribution, and effects of inhibitors, J. Neurochem. 47 (1986) 1376–1386.
[25] L. Tretter, V. Adam-Vizi, Generation of reactive oxygen species in the reaction catalyzed by alpha-ketoglutarate dehydrogenase, J. Neurosci. 24 (2004) 7771–7778.
[26] K.E. Akerman, M.K. Wikstrom, Safranine as a probe of the mitochondrial membrane potential, FEBS Lett. 68 (1976) 191–197.
[27] T.R. Figueira, D.R. Melo, A.E. Vercesi, R.F. Castilho, Safranine as a fluorescent probe for the evaluation of mitochondrial membrane potential in isolated organelles and permeabilized cells, Methods Mol. Biol. 810 (2012) 103–117.
[28] A. Saito, R.F. Castilho, Inhibitory effects of adenine nucleotides on brain mitochondrial permeability transition, Neurochem. Res. 35 (2010) 1667–1674.
[29] A.J. Kowaltowski, A.E. Vercesi, R.F. Castilho, Mitochondrial membrane protein thiol reactivity with N-ethylmaleimide or mersalyl is modified by Ca2+: correlation with mitochondrial permeability transition, Biochim. Biophys. Acta 1318 (1997) 395–402.

[30] T. Mosmann, Rapid colorimetric assay for cellular growth and survival: application to proliferation and cytotoxicity assays, J. Immunol. Methods 65 (1983) 55–63.
[31] M.M. Bradford, A rapid and sensitive method for the quantitation of microgram quantities of protein utilizing the principle of protein-dye binding, Anal. Biochem. 72 (1976) 248–254.
[32] J.G. Pastorino, G. Simbula, K. Yamamoto, P.A. Glascott Jr., R.J. Rothman, J.L. Farber, The cytotoxicity of tumor necrosis factor depends on induction of the mitochondrial permeability transition, J. Biol. Chem. 271 (1996) 29792–29798.
[33] K.M. Broekemeier, J.R. Iben, E.G. LeVan, E.D. Crouser, D.R. Pfeiffer, Pore formation and uncoupling initiate a Ca2 + −independent degradation of mitochondrial phospholipids, Biochemistry 41 (2002) 7771–7780.
[34] M. Nishimura, Y. Okimura, H. Fujita, H. Yano, J. Lee, E. Suzaki, M. Inoue, K. Utsumi, J. Sasaki, Mechanism of 3-nitropropionic acid-induced membrane permeability transition of isolated mitochondria and its suppression by L-carnitine, Cell Biochem. Funct. 26 (2008) 881–891.
[35] C. Chinopoulos, A.A. Starkov, G. Fiskum, Cyclosporin A-insensitive permeability transition in brain mitochondria: inhibition by 2-aminoethoxydiphenyl borate, J. Biol. Chem. 278 (2003) 27382–27389.
[36] P. Costantini, B.V. Chernyak, V. Petronilli, P. Bernardi, Modulation of the mitochondrial permeability transition pore by pyridine nucleotides and dithiol oxidation at two separate sites, J. Biol. Chem. 271 (1996) 6746–6751.
[37] V. Petronilli, P. Costantini, L. Scorrano, R. Colonna, S. Passamonti, P. Bernardi, The voltage sensor of the mitochondrial permeability transition pore is tuned by the oxidation-reduction state of vicinal thiols. Increase of the gating potential by oxidants and its reversal by reducing agents, J. Biol. Chem. 269 (1994) 16638–16642.
[38] T.S. Kim, D.W. Jeong, B.Y. Yun, I.Y. Kim, Dysfunction of rat liver mitochondria by selenite: induction of mitochondrial permeability transition through thiol-oxidation, Biochem. Biophys. Res. Commun. 294 (2002) 1130–1137.
[39] F. Eichler, W.H. Tan, V.E. Shih, P.E. Grant, K. Krishnamoorthy, Proton magnetic resonance spectroscopy and diffusion-weighted imaging in isolated sulfite oxidase deficiency, J. Child Neurol. 21 (2006) 801–805.
[40] A. Kelly, C.A. Stanley, Disorders of glutamate metabolism, Ment. Retard. Dev. Disabil. Res. Rev. 7 (2001) 287–295.
[41] P.B. Mills, E.J. Footitt, S. Ceyhan, P.J. Waters, C. Jakobs, P.T. Clayton, E.A. Struys, Urinary AASA excretion is elevated in patients with molybdenum cofactor deficiency and isolated sulphite oxidase deficiency, J. Inherit. Metab. Dis. 35 (2012) 1031–1036.
[42] E.A. Struys, B. Nota, A. Bakkali, S. Al Shahwan, G.S. Salomons, B. Tabarki, Pyridoxine-dependent epilepsy with elevated urinary alpha-amino adipic semialdehyde in molybdenum cofactor deficiency, Pediatrics 130 (2012) e1716–e1719.
[43] C.L. Moore, Specific inhibition of mitochondrial Ca++ transport by ruthenium red, Biochem. Biophys. Res. Commun. 42 (1971) 298–305.
[44] C. Yarana, J. Sripetchwandee, J. Sanit, S. Chattipakorn, N. Chattipakorn, Calcium-induced cardiac mitochondrial dysfunction is predominantly mediated by cyclosporine A-dependent mitochondrial permeability transition pore, Arch. Med. Res. 43 (2012) 333–338.
[45] G. Hajnoczky, G. Csordas, S. Das, C. Garcia-Perez, M. Saotome, S. Sinha Roy, M. Yi, Mitochondrial calcium signalling and cell death: approaches for assessing the role of mitochondrial Ca2+ uptake in apoptosis, Cell Calcium 40 (2006) 553–560.
[46] D.B. Zorov, M. Juhaszova, Y. Yaniv, H.B. Nuss, S. Wang, S.J. Sollott, Regulation and pharmacology of the mitochondrial permeability transition pore, Cardiovasc. Res. 83 (2009) 213–225.
[47] M. Zoratti, I. Szabo, The mitochondrial permeability transition, Biochim. Biophys. Acta 1241 (1995) 139–176.
[48] A. Rasola, P. Bernardi, Mitochondrial permeability transition in Ca(2+)-dependent apoptosis and necrosis, Cell Calcium 50 (2011) 222–233.
[49] J. Pottecher, M. Guillot, E. Belaidi, A.L. Charles, A. Lejay, A. Gharib, P. Diemunsch, B. Geny, Cyclosporine A normalizes mitochondrial coupling, reactive oxygen species production, and inflammation and partially restores skeletal muscle maximal oxidative capacity in experimental aortic cross-clamping, J. Vasc. Surg. 57 (2013) 1100–1108 (e1102).
[50] E. Basso, L. Fante, J. Fowlkes, V. Petronilli, M.A. Forte, P. Bernardi, Properties of the permeability transition pore in mitochondria devoid of Cyclophilin D, J. Biol. Chem. 280 (2005) 18558–18561.
[51] G.P. McStay, S.J. Clarke, A.P. Halestrap, Role of critical thiol groups on the matrix surface of the adenine nucleotide translocase in the mechanism of the mitochondrial permeability transition pore, Biochem. J. 367 (2002) 541–548.
[52] A.P. Halestrap, K.Y. Woodfield, C.P. Connern, Oxidative stress, thiol reagents, and membrane potential modulate the mitochondrial permeability transition by affecting nucleotide binding to the adenine nucleotide translocase, J. Biol. Chem. 272 (1997) 3346–3354.
[53] M. Crompton, Mitochondrial intermembrane junctional complexes and their role in cell death, J. Physiol. 529 (Pt 1) (2000) 11–21.
[54] P.X. Petit, M. Goubern, P. Diolez, S.A. Susin, N. Zamzami, G. Kroemer, Disruption of the outer mitochondrial membrane as a result of large amplitude swelling: the impact of irreversible permeability transition, FEBS Lett. 426 (1998) 111–116.
[55] D.R. Green, J.C. Reed, Mitochondria and apoptosis, Science 281 (1998) 1309–1312.
[56] J.W. Olney, C.H. Misra, T. de Gubareff, Cysteine-S-sulfate: brain damaging metabolite in sulfite oxidase deficiency, J. Neuropathol. Exp. Neurol. 34 (1975) 167–177.
[57] B. Kagedal, M. Kallberg, B. Sorbo, A possible involvement of glutathione in the detoxication of sulfite, Biochem. Biophys. Res. Commun. 136 (1986) 1036–1041.